NASA/TM–20220019279

Improvement of Pressure Sensitive Paint in a Cryogenic Oxygen-Poor Environment

A. Neal Watkins and Daniel Reese
Langley Research Center, Hampton, Virginia

October 2023

NASA STI Program Report Series

Since its founding, NASA has been dedicated to the advancement of aeronautics and space science. The NASA scientific and technical information (STI) program plays a key part in helping NASA maintain this important role.

The NASA STI program operates under the auspices of the Agency Chief Information Officer. It collects, organizes, provides for archiving, and disseminates NASA's STI. The NASA STI program provides access to the NTRS Registered and its public interface, the NASA Technical Reports Server, thus providing one of the largest collections of aeronautical and space science STI in the world. Results are published in both non-NASA channels and by NASA in the NASA STI Report Series, which includes the following report types:

- TECHNICAL PUBLICATION. Reports of completed research or a major significant phase of research that present the results of NASA Programs and include extensive data or theoretical analysis. Includes compilations of significant scientific and technical data and information deemed to be of continuing reference value. NASA counterpart of peer-reviewed formal professional papers but has less stringent limitations on manuscript length and extent of graphic presentations.

- TECHNICAL MEMORANDUM. Scientific and technical findings that are preliminary or of specialized interest, e.g., quick release reports, working papers, and bibliographies that contain minimal annotation. Does not contain extensive analysis.

- CONTRACTOR REPORT. Scientific and technical findings by NASA-sponsored contractors and grantees.

- CONFERENCE PUBLICATION. Collected papers from scientific and technical conferences, symposia, seminars, or other meetings sponsored or co-sponsored by NASA.

- SPECIAL PUBLICATION. Scientific, technical, or historical information from NASA programs, projects, and missions, often concerned with subjects having substantial public interest.

- TECHNICAL TRANSLATION. English-language translations of foreign scientific and technical material pertinent to NASA's mission.

Specialized services also include organizing and publishing research results, distributing specialized research announcements and feeds, providing information desk and personal search support, and enabling data exchange services.

For more information about the NASA STI program, see the following:

- Access the NASA STI program home page at http://www.sti.nasa.gov

- Help desk contact information:

https://www.sti.nasa.gov/sti-contact-form/
and select the "General" help request type.

NASA/TM–20220019279

Improvement of Pressure Sensitive Paint in a Cryogenic Oxygen-Poor Environment

A. Neal Watkins and Daniel Reese
Langley Research Center, Hampton, Virginia

National Aeronautics and
Space Administration

Langley Research Center
Hampton, Virginia
23681-2199

October 2023

Available from:

NASA STI Program / Mail Stop 148

NASA Langley Research Center

Hampton, VA 23681-2199

Fax: 757-864-6500

Improvement of Pressure Sensitive Paint in a Cryogenic Oxygen-Poor Environment

A. Neal Watkins[1] and Daniel Reese[2]
NASA Langley Research Center, Hampton, VA 23681, USA

This report details specific improvements to the use of Pressure Sensitive Paint (PSP) in an oxygen-poor environment, with an emphasis on cryogenic PSP in the National Transonic Facility (NTF). For this work, several improvements to the application of PSP and data acquisition have been investigated in the 0.3-m Transonic Cryogenic Tunnel (generally considered a pilot facility for the NTF) and these results will be presented. In addition, several improvements to the existing PSP system at NTF are presented as well as a brief section on further improvements that can be investigated.

I. Introduction

The accurate determination of spatially continuous pressure distributions on aerodynamic surfaces is critical for the understanding of complex flow mechanisms and for comparison with computational fluid dynamics (CFD) predictions. Most conventional pressure measurements are based on the use of pressure taps and electronically scanned pressure transducers. While these approaches provide accurate pressure information, they are limited to providing data at discrete points. Moreover, the integration of a sufficient number of these devices on a surface can be time and labor intensive and can bear a significant cost.

The Pressure Sensitive Paint (PSP) technique allows for the accurate determination of pressure distributions over an aerodynamic surface and is based on an emitted signal from a luminescent coating. However, when full flight Reynolds number measurements are required, it is common to use a cryogenic facility, especially if an increase in model size to full-scale is not a viable option. Without a full-scale model, sub-scale models require higher Reynolds numbers in the wind tunnel facility to match the full-scale flight conditions. One way to achieve these higher Reynolds number conditions is to cool the tunnel fluid medium to cryogenic conditions, which can increase the wind tunnel Reynolds number by as much as a factor of 7 with no increase in dynamic pressure and with a reduction in drive power [1]. However, in these conditions, several challenges arise when trying to employ PSP.

This report will detail several methods that can improve the operation and performance of the existing PSP system in NTF. This includes potential improvements to the measurement technique itself at cryogenic conditions as well as improvements to the existing equipment. Investigation of the measurement improvements was conducted at the NASA Langley (LaRC) 0.3-m Transonic Cryogenic Tunnel (0.3-m TCT), which is a small-scale cryogenic facility often considered as a pilot facility for investigating measurement techniques before deploying to the NTF. The results from these tests will be presented as well as potential further improvement areas. Finally, this report is being submitted in fulfillment of Milestone TTT.L2.L.05.22.1 (Pressure Sensitive Paint Low Oxygen Environment Facility Demonstration) in support of the Reduced Life Cycle Cost (RLCC) Sub-Project and Innovative Measurements (IM) Enduring Discipline Research Area under the Transformational Tools and Technologies (T^3) Project.

---

[1] Aerospace Science Technologist, Advanced Measurement and Data Systems Branch.

[2] Aerospace Science Technologist, Advanced Measurement and Data Systems Branch.

II. Pressure Sensitive Paint

The PSP technique [2-6] exploits the oxygen sensitivity of luminescent probe molecules suspended in gas-permeable binder materials. When a luminescent molecule absorbs a photon, it transitions to an excited singlet energy state. The molecule can then recover to the ground state by the emission of a photon of a longer wavelength, known as a radiative process. However, certain of these luminescent materials can also interact with an oxygen molecule such that the transition back to the ground state is non-radiative in a process known as collisional quenching. The rate at which these two processes (radiative vs. non-radiative) compete is dependent on the concentration of oxygen present and can be described by the Stern-Volmer relationship [7]

$$I_0/I = 1 + K_{SV}(T)P_{O_2} \tag{1}$$

where I_0 is the luminescence intensity in the absence of O_2 (i.e., vacuum), I is the luminescence intensity at some partial pressure of oxygen (P_{O2}), and K_{SV} is the Stern-Volmer constant, which is dependent on temperature (T).

There are several issues with this relationship, especially in regard to wind-tunnel applications. First, it is a practical impossibility to measure I_0 in a wind tunnel application. Second, the luminescent signal from the paint is not only a function of pressure, it also varies with factors such as illumination intensity, probe molecule concentration, and paint layer thickness. These spatial variations typically result in a non-uniform luminescence signal from the painted surface. The spatial variations are usually eliminated by taking a ratio of the luminescent intensity of the paint at the test condition with the luminescent intensity of the paint at a known reference condition usually at wind-off. Thus Eq. (1) can be cast into a more suitable form

$$I_{REF}/I = A(T) + B(T) * (P/P_{REF}) \tag{2}$$

where I_{REF} is the recovered luminescence intensity at a reference pressure, P_{REF}. The coefficients $A(T)$ and $B(T)$ are for a given PSP formulation and are usually determined beforehand using laboratory calibration procedures.

From Eq. (1) it can be seen that conducting PSP measurements in oxygen-poor environments can be difficult since PSP depends on the partial pressure of O_2. This can be further exacerbated if these types of measurements are required in a cryogenic environment. This is due to both the low oxygen environment in the nitrogen atmosphere and the fact that the diffusion of O_2 into the PSP binder is highly temperature dependent, and at cryogenic temperatures, is practically non-existent.

For the cryogenic testing case, the most commonly employed PSP binder that can be applied to a model using conventional paint application techniques is based on using poly[1-(trimethylsilyl)-1-propyne (PTMSP), which was independently developed at both NASA Langley [8] and the National Aerospace Laboratory in Japan [9, 10]. PTMSP is used as it is a glassy polymer with a large free volume, enabling it to have a very high oxygen diffusion rate [11]. This formulation has been previously used at 0.3-m TCT [8, 12], NTF [13, 14], and other facilities [9, 10, 15].

III. Experimental

A. 0.3-m TCT

All wind tunnel testing was carried out in the NASA LaRC 0.3-m TCT. The 0.3-m TCT is a continuous-flow, single-return, fan-driven transonic tunnel which can employ either air (ambient temperature testing) or nitrogen (cryogenic temperature testing) as the test medium. It is capable of operating at stagnation temperatures from about 100 K to about 322 K and stagnation pressures from slightly greater than 101 kPa to 607 kPa. Test section Mach number can be varied from near 0 to 0.9. The ability to operate at cryogenic temperatures and high pressure provides an extremely high Reynolds number capability at relatively low model loadings. The test section has computer-controlled angle-of-attack and traversing-wake-survey rake systems. Two inches of honeycomb and five anti-turbulence screens in the settling chamber provide flow quality suitable for natural laminar flow testing. The relevant characteristics for the 0.3-m TCT are shown in Table 1, and additional design features and characteristics regarding the cryogenic concept in general (and the 0.3-m TCT in particular) can be found in works by Kilgore, *et al.* [16] and Kilgore [17].

Table 1 Relevant characteristics of the 0.3-m TCT

Test section dimensions	0.33 m by 0.33 m
Speed	Mach 0.1 to 0.9
Reynolds Number	3.3 to 330 x 10^6 per m
Temperature	100 to 322 K
Pressure	101 to 607 kPa
Test gas	Nitrogen or air

B. Instrumentation

Illumination

Illumination was achieved using commercially available light-emitting diode (LED) arrays (Innovative Scientific Solutions, Inc. (ISSI), http://innssi.com) These arrays were designed specifically for PSP and TSP (temperature sensitive paint) applications, thus are capable of producing a very stable output of more than 3W with 0.1% drift per hour after warm-up. For this work, the LEDs were configured to emit at 400 nm with a 20 nm bandwidth at full width at half maximum (FWHM).

Image Acquisition

Optical images were acquired using either one of two cameras. The first camera employed was a PSP-CCD-M CCD camera (ISSI) having a resolution of 1600 x 1200 pixels operating at either 12-bit or 14-bit resolution. The camera is interfaced to the computer via gigabit Ethernet (GIG-E) and capable of acquiring data up to 44 frames per second. The second camera was a CoolSNAP HQ CCD camera (Photometrics), which is a thermoelectrically cooled CCD having a resolution of 1392 x 1040 pixels and operates with 12-bit resolution. Both of these CCD cameras are interline-transfer cameras.

Illumination and Image Acquisition Mounting in 0.3-m TCT

The optical access for the 0.3-m TCT consists of a "D-shaped" window that was originally designed for off-body flow visualization studies. The D-shaped window is constructed of Schlieren quality fused silica that is mounted in the upper half of the circular angle-of-attack turntables. For this work, the airfoil is centered horizontally in the test section with its centerline 1.9 cm below the lower edge of the window. As such, there is no direct optical access to the surface. A diagram of the D-shaped window with a generic airfoil is shown in Fig. 1 [18]. In addition, the D-shaped window (and test section) is separated from the outside of the tunnel by a rectangular pressure plenum. To facilitate illumination and image acquisition, a pair of mirrors were deployed as a periscope to allow optical access to the upper surface of the model. This periscope was attached to the test section door inside the plenum. A photograph of the optical setup is shown in Fig. 2(a).

Optical access from outside of the plenum is provided by a window placed in the plenum wall. This window is also made of Schlieren quality fused silica with a diameter of 22.9 cm. To keep the outer window clear of condensation (due to the large temperature difference on either side of the window), a large canister with a purge ring is connected to the plenum. The camera and the LEDs were placed in this canister. The canister mounted to the plenum is shown in Fig. 2(b).

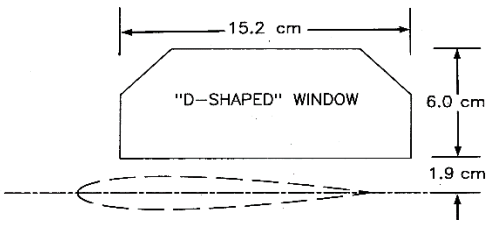

Fig. 1 Geometry of the "D-shaped" window with a generic airfoil showing approximate location. From Ref. [18]

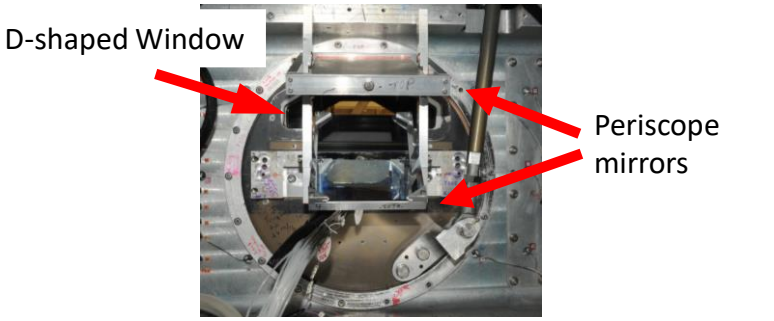

(a)

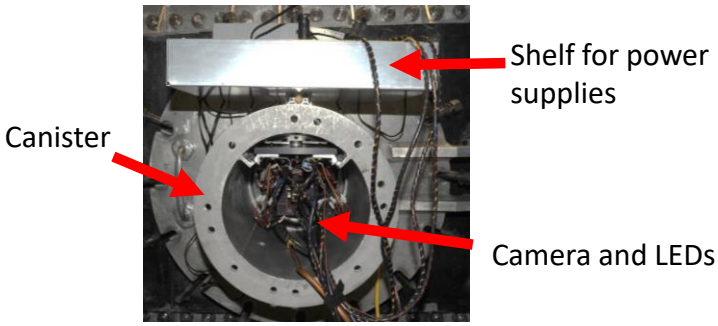

(b)

Fig. 2 Mounting of equipment at 0.3-m TCT: (a) Optical setup showing the "D-shaped: window and the periscope assembly; (b) Canister mounted onto the side of the tunnel containing the camera and LED illumination sources.

Model

The airfoil model used for the 0.3-m TCT wind tunnel work is designated as the NASA SC(3)-0712(B) [19]. The model is a supercritical airfoil with a 0.7 design lift coefficient and is 12% thick. The airfoil has a chord of 15.24 cm (6.0 in) and is constructed from VascoMax C-200 steel. The airfoil also contained 74 pressure transducers on the upper surface, with approximately 40 visible in the PSP images.

Oxygen Introduction and Monitoring

As described in Section II, PSP measures the partial pressure of O_2. Thus, O_2 must be present in the flow for PSP to be effective. However, in cryogenic conditions, the test medium is typically nitrogen, which generally contains a very small amount of O_2 (less than 50 ppm depending on grade). Therefore, to use PSP in these conditions, some O_2 must be injected to increase its concentration. For this test, the concentration of O_2 was increased using cylinders of dry air. The air was introduced to the flow just aft of the test section through a pre-existing feed-through. To keep the air from freezing at the feed-through, the line was heated using a heater tape. The flow was activated remotely from the control room using a solenoid valve. The air insertion equipment is shown in Fig. 3. With this configuration, the O_2 concentration in the flow could be increased from ~20 ppm (native with no air introduction) to several thousand ppm depending on tunnel conditions. For this work, the data was generally collected at O_2 concentration ranges from 1000-5000 ppm to more generally align with what is traditionally used at NTF.

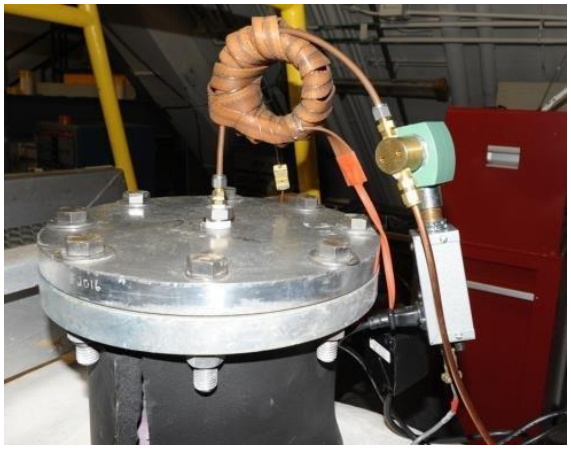

Fig. 3 Air insertion line showing heating tape (to keep air from freezing upon injection) and solenoid for remote operation.

In order to monitor the actual O_2 concentration in the tunnel, a solid-state electrochemical O_2 sensor was introduced. The sensor chosen was the OX-5 (Panametrics) sensor, which is a galvanic fuel cell that is designed to measure O_2 concentration ranges from 0 – 10,000 ppm (other options can be purchased for extending the range). These types of sensors are self-contained and require no electrolyte to change or electrodes to clean. The sensor was controlled using a Panametrics oxy.IQ Oxygen Transmitter. The transmitter was interfaced to the 0.3-m TCT prior to the test section (through another pre-existing feed through) and a vacuum pump was employed to ensure that the oxygen sensor experienced the required flow rate (500 cm^3/min). The oxygen sensor was designed for simply monitoring the oxygen content in the flow, so a video camera was employed to observe the transmitter unit from the control room.

Data Acquisition

One of the goals of this project was to evaluate the efficacy of using alternative data acquisition techniques to improve efficiency in the NTF. Traditionally, PSP data acquired at NTF has employed the radiometric method, in which reference images at wind-off (or very low speed) conditions are collected as the I_{REF} term in Eq. (2). Then wind-on images (at appropriate tunnel conditions) are acquired as the I term. To minimize the effects of model alignment and illumination terms, the wind-off images are required at each model position in the tunnel. Furthermore, the wind-off images are collected as close in time as possible to the wind-on images due to potential paint degradation effects that could occur. This can add significant time for testing, as essentially a test matrix must be run twice.

A second method of PSP data acquisition is known as "lifetime-based" (or simply "lifetime") PSP. In the lifetime-based technique, excitation of the PSP is accomplished using a modulated light source (e.g., laser, flash lamp, or pulsed LED arrays). A fast-framing camera (intensified CCD or interline transfer CCD) is used to collect the excited state luminescence decay. Typically, the decay is approximated by acquiring two or more images at different delay times during and/or after the pulsed excitation and integrating photons for fixed periods of time (i.e., gate widths) that have been predetermined to maximize the pressure sensitivity. A graphical representation of the lifetime technique is shown in Fig. 4. The first image (Gate 1) is usually collected either during the excitation pulse or shortly after it ends. The second image (Gate 2) is taken a short time after Gate 1, and is generally after the excitation pulse, maximizing pressure sensitivity. The lifetime-based approach employing interline CCD cameras and pulsed LED arrays has been used at many different facilities.

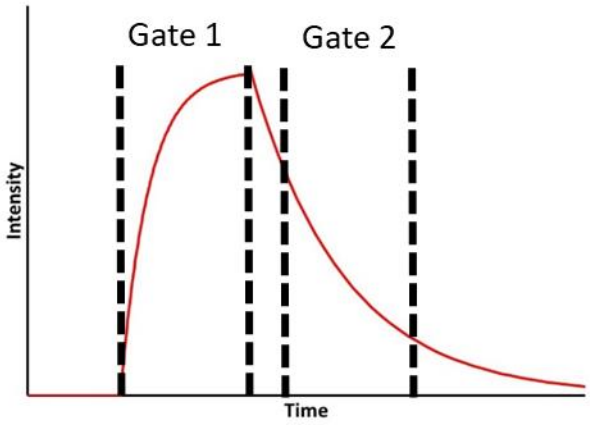

Fig. 4 Graphical representation of the lifetime-based PSP data acquisition technique.

For this work, interline transfer cameras were chosen to facilitate use of the lifetime-based technique and the LED arrays are capable of being pulsed quickly (as low as 10 μs pulse widths at rates up to 5 kHz). The interline transfer cameras were also equipped with a "frame accumulation" mode, which allowed for the collection of multiple light pulses which were added together to provide sufficient signal-to-noise for a single gate image. For example, with the frame accumulation mode, it was possible to collect several thousand light pulses for a respective gate image.

Results

A. Results with the PSP-CCD-M camera

The first camera that was evaluated for the traditional lifetime-based data acquisition was the ISSI PSP-CCD-M. It is a small interline transfer CCD camera that has a similar form factor as the existing CCD cameras currently in use at the NTF. The PSP-CCD-M camera is shown in Fig. 5.

Fig. 5 Photograph of the PSP-CCD-M Interline transfer CCD camera.

For simplicity, and since this report is not concerned with the actual aerodynamics of the SC(3)-0712(B) airfoil, discussion of the data will be limited to only a few conditions. Similar trends are seen throughout the data. The data quality from the camera was assessed and representative images are shown in Fig. 6. Images were acquired using both the frame accumulation mode for lifetime (Fig. 6(a) and Fig. 6(b)) as well as the more standard intensity method in which a longer LED pulse was used with no accumulation of the light (Fig. 6(c)). This is analogous to a standard radiometric approach using wind-on and slow-roll images.

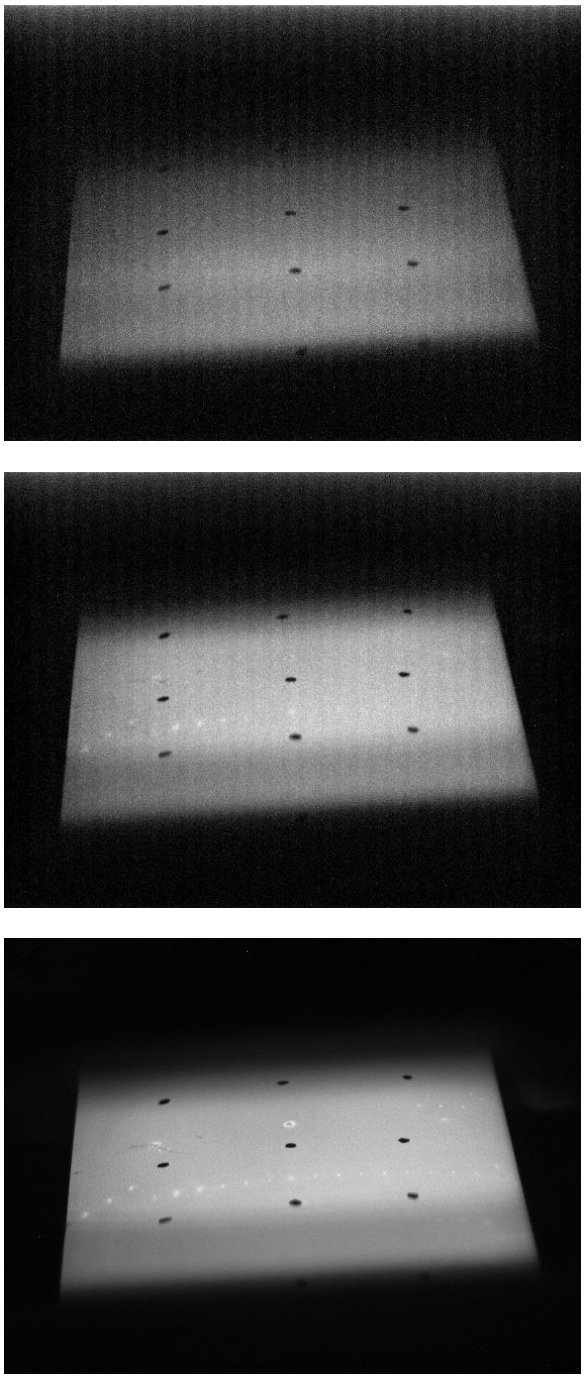

a)

b)

c)

Fig. 6 Representative images from the ISSI PSP-CCD-M. a) Frame accumulation image (gate 1) collected at 116 K (-250 °F), M = 0.7, AOA = 4 deg.; b) Frame accumulation mode image (gate 1) collected at 250 K (-10 °F), M = 0.7, AOA = 4 deg.; c) traditional long exposure (no frame accumulation) collected at 250 K (-10 °F), M=0.7, AOA = 4 deg.

Several observations about the images shown in Fig. 6 are readily apparent. First, the noise in the frame accumulation mode images (Fig. 6(a) and 6(b)) are significantly higher than the non-frame accumulation image (Fig. 6(c)). This is seen as the "popcorn" like effect in the images. This is most likely due to the fact that the PSP-CCD-M camera is not thermoelectrically cooled, and this is shot noise that is magnified due to the very short exposures. The second observation is the presence of vertical "bands" in the frame accumulation images. This banding is fixed pattern

noise that is associated with the frame transfer process itself. It is essentially the masked area that is used to transfer the charge on the CCD so that the second image can be acquired. Unfortunately, while this may be a fixed pattern, the intensity of the artifact is not constant. It is camera dependent but can also vary across the chip of a single camera. Thus, there is no good way to filter out this type of noise. A potential solution to this issue will be described in a later section of this report.

For the higher noise levels in the frame accumulation mode, a simple background subtraction can remove much of this noise by acquiring an image using the same timing settings that are used for the frame accumulation images without firing the LEDs. A comparison of the results before and after background subtraction are shown in Fig. 7. It is apparent that much of the noise due to pixel response can be corrected, but the banding due to the interline transfer process of the camera is still present.

Original

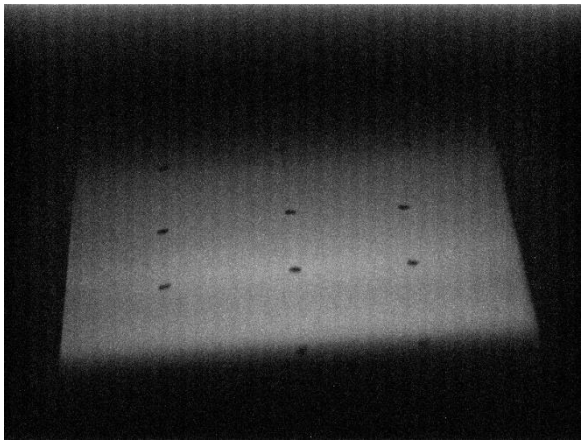

After Background Subtraction

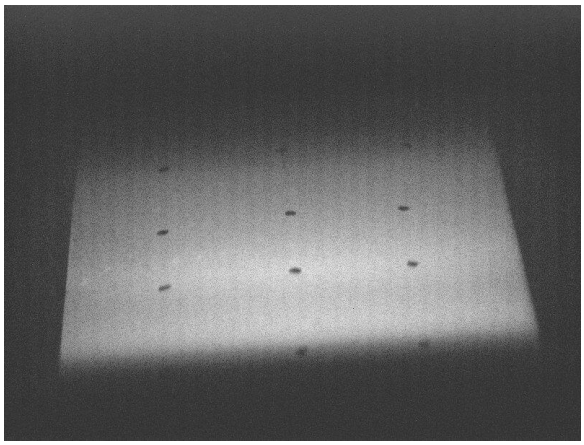

Fig. 7 Comparison of original Gate 1 image at 116 K before (top) and after (bottom) background subtraction.

Processing of these images was problematic in that even with background subtraction, noise in the readout overwhelms any usable quantitative data in the images. For completeness, this data was still analyzed. The typical simplified analysis involves dividing the Gate 1 image by the Gate 2 image (with Gate 1 being taken during the LED pulse and Gate 2 directly after the LED pulse, this is analogous to I_{REF} and I in Eq. 2). However, in the lifetime acquisition approach in PSP, it is often desirable to have another reference image pair, typically taken at wind-off or slow-roll conditions. This can account for factors such as paint inhomogeneity, which can greatly affect the PSP calculations, especially in cases where small signal changes are expected (e.g., low speed or oxygen poor environments). Variations of this type of data analysis are done when using the technique in both transonic [20] and cryogenic [15] lifetime PSP. In this case, another image pair was acquired at a slow-roll condition (M = 0.183, close to the slowest stable speed that 0.3-m TCT can operate) under similar oxygen levels. The ratio of the images collected at the wind-on conditions was then divided by the ratio obtained at the slow-roll condition. Finally, the ratioed images (without and with the slow-roll condition) were fit to pressure taps on the model, and the results are shown in Fig. 8.

As can be seen, the data is extremely noisy, bordering on unusable. These results are most likely due to a combination of two factors:

1) The fact that the PSP-CCD-M camera is not thermoelectrically cooled. This significantly increases the pixel shot noise, which is dominant in the images
2) The optical setup of the 0.3-m TCT. This precludes the ability to illuminate the surface with as much light as possible (because the LEDs must also be projected through the periscope) and the large grazing angle of the camera.

These factors led to the need for a large number of pulses (leading to higher shot noise) to achieve suitable images. In addition, to maintain a short enough data acquisition window for the tunnel, only a single pair of images could be acquired. Thus, the ability to try and improve the signal-to-noise ratio even a minimal amount is not possible.

Standard Gate 1/Gate 2

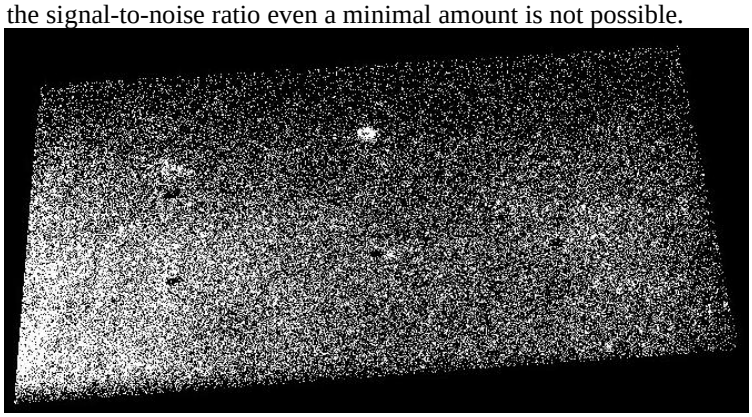

Ratio-of-Ratios (using slow roll image pair)

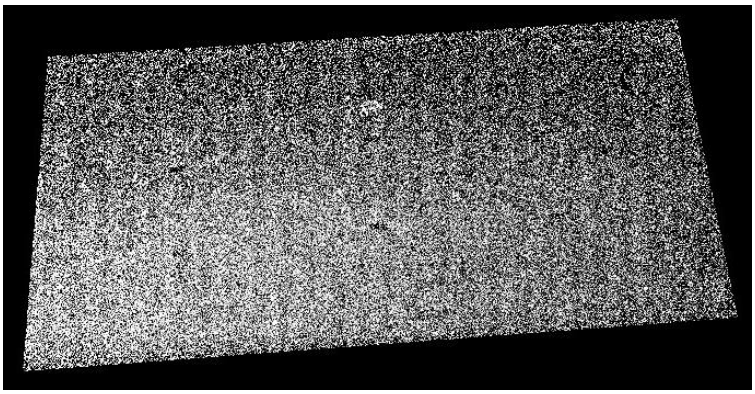

Fig. 8 Data analysis for the lifetime images collected using the frame accumulation mode with the PSP-CCD-M camera. The top image is the standard Gate 1/Gate 2 analysis, and the bottom image is the analysis using a slow-roll image pair for reference. Tunnel conditions were as follows: T= 116 K, M = 0.7, AOA = 4 deg. Tunnel flow is from right to left in the images.

Standard intensity-based data acquisition was also employed for comparison with the frame-accumulation lifetime results. In this case, the temperature of the tunnel was 250 K as this was done near the end of the test (to maximize efficiency, the 0.3-m TCT is typically run from coldest temperature to warmest temperature). Similar to the lifetime data acquisition, the reference image is acquired at a slow-roll condition to maintain mixing of the oxygen in the tunnel. Analysis of this data was similar to the lifetime data, except that an additional step of correlating the wind-on image with the slow-roll image is required. This will account for minor differences in position but does not account for any changes in illumination that may have occurred due to the airfoil being in a slightly different light field between the images. The PSP results are shown in Fig. 9.

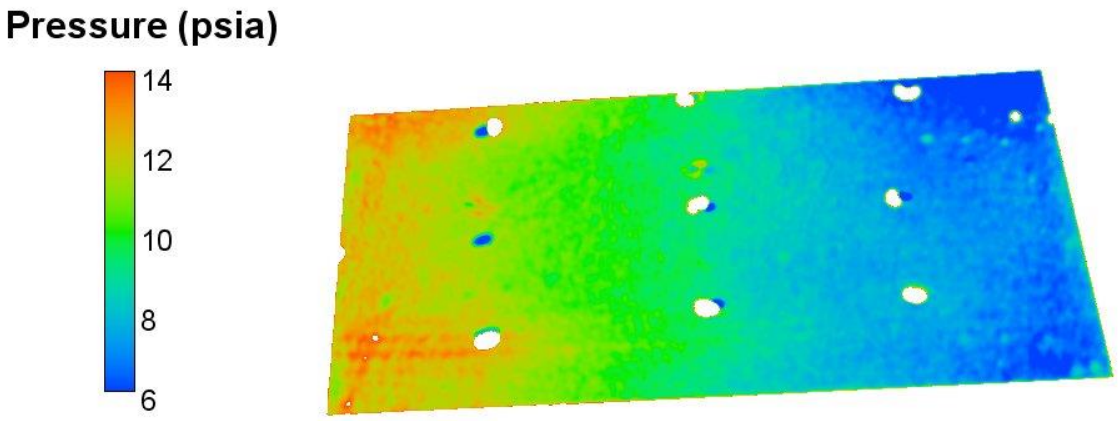

Fig. 9 Recovered pressure using PSP from PSP-CCD-M camera in intensity mode. Test conditions were T = 250 K, M = 0.7, AOA = 4 deg. Tunnel flow is from right to left in the image.

As shown in Fig. 9, the results are much better than the images obtained while operating in the frame accumulation mode (Fig. 8). This data was taken with only one image at wind-off and one image at the slow-roll condition (to be consistent with the frame accumulation mode images), so significantly increased signal-to-noise can be obtained by averaging images. In addition, the quality of the images is still affected by the optical setup that is available in the 0.3-m TCT.

Results with the CoolSNAP HQ Camera

The second camera that was evaluated for the traditional lifetime-based data acquisition was the Photometrics CoolSNAP HQ CCD camera. This is a larger CCD camera equipped with thermoelectric cooling and is one of the first CCD cameras of this type that was equipped with a frame accumulation mode (named a hardware accumulator by Photometrics). This camera was used previously in the first lifetime experiments performed at NASA Langley [21] and has been supplanted by a newer generation of cameras (CoolSNAP K4) currently employed in facilities such as AEDC, NASA Ames 11-Foot Tunnel, and the NASA Langley Unitary Plan Wind Tunnel.

For this testing, the PSP-CCD-M camera was replaced with the CoolSNAP. Due to the size differences between the cameras, slight changes in the both the imaging and excitation fields were present. Unfortunately, during this portion of the test, the angle-of-attack system for the 0.3-m TCT suffered several issues resulting in an inability to move, especially at the coldest temperature (116 K). To minimize this, the temperature of the tunnel was raised to 150 K (-190 °F) which allowed movement to 3.2 deg. This is as close to 4 deg that the model system could reach.

The collected Gate 1 image is shown in Fig. 10. As can be seen, the image is much less noisy than the PSP-CCD-M camera (seen in Fig. 7) most likely due to the thermoelectric cooling available on the CoolSNAP (the CoolSNAP CCD is cooled to 243 K (-22 °F) compared with no cooling on the PSP-CCD-M). The clarity of the image implies that cooling the chip significantly reduces the shot noise from the camera.

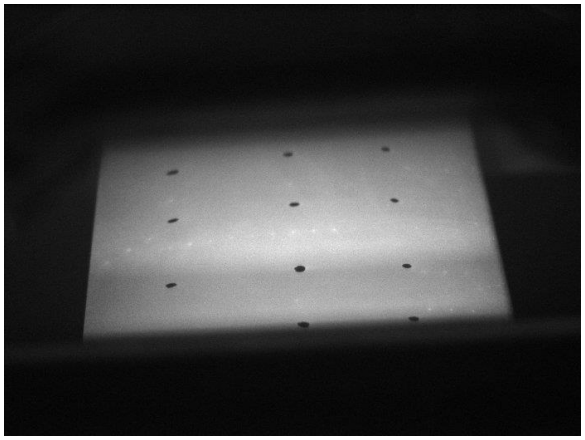

Fig. 10 Gate 1 image collected in frame accumulation mode on the CoolSNAP HQ camera.

Data analysis for the lifetime images was done in a fashion similar to the images collected with the PSP-CCD-M camera. The initial analysis was to simply calculate a ratio of the Gate 1 and Gate 2 images and calibrating using the existing pressure taps. This is shown in Fig. 11. The image is cast in greyscale to show that the image is dominated by paint application features (such as swirls and streaks). As mentioned above, this is due to paint inhomogeneity that is imparted due to paint spraying, different paint thickness, luminescent dye concentration gradients, etc. These factors are often present, but their effect is greatly exacerbated when trying to measure small oxygen concentration changes (such as low speed or oxygen poor environments).

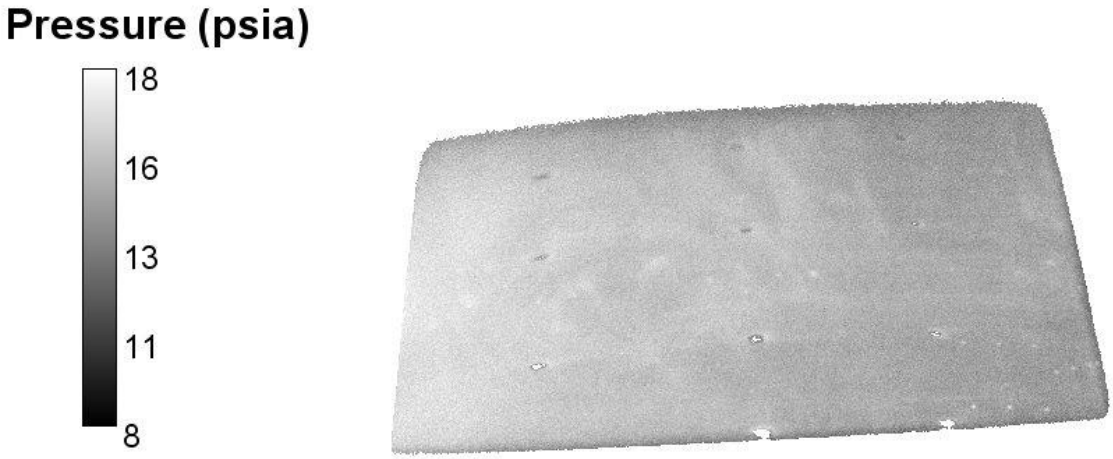

Fig. 11 Recovered pressure from CoolSNAP camera in lifetime mode using only wind-on Gate 1 and Gate 2 images. Test conditions are T = 150 K, M = 0.7, AOA = 3.2 deg. Tunnel flow is from right to left in the image.

Correcting for this requires the use of reference images, often acquired at similar oxygen levels but at wind-off or slow-roll conditions. The paint inhomogeneity is a constant factor, thus, this process can correct for these effects. This is often called the "ratio-of-ratios" technique as both the wind-on and the reference image are constructed from a ratio of Gate 1 and Gate 2 images. Analysis of the data in Fig. 11 using a reference lifetime image at a slow-roll is shown in Fig. 12. In this image, the separation region near the leading edge is clearly visible, and aft of the region, the pressure

gradually increases as expected. However, the image still suffers from noise due to the optical access limitation and small changes in intensities due to the oxygen poor environment.

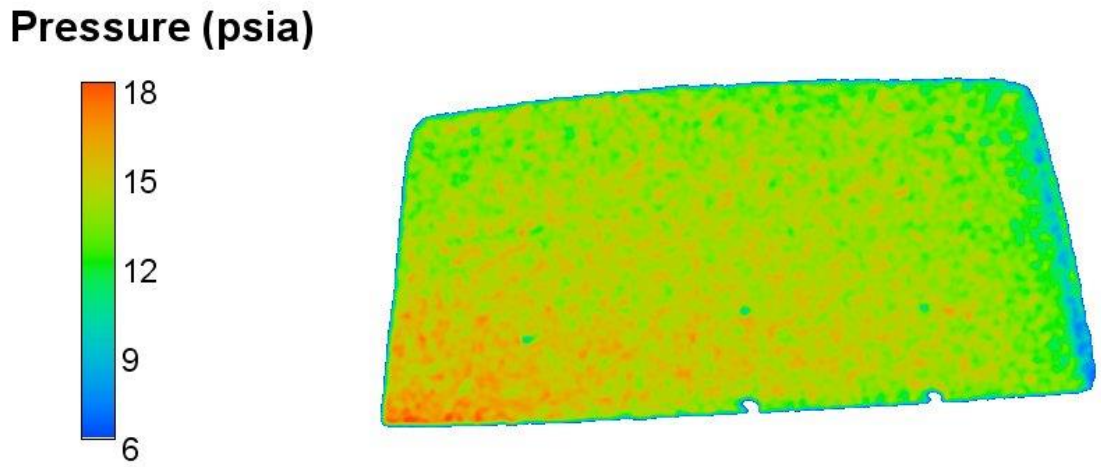

Fig. 12 Recovered pressure from CoolSNAP camera in lifetime mode using the ratio-of-ratios technique. Test conditions are T = 150 K, M = 0.7, AOA = 3.2 deg. Tunnel flow is from right to left in the image.

For completeness, an intensity analysis was also completed for this data set. However, due to time limitations, a set of longer integration intensity images was not acquired as with the PSP-CCD-M camera. In this case, the intensity image is simply a ratio of the Gate 2 slow-roll image and the Gate 2 wind-on image. These results are shown in Fig. 13. Similar trends with the lifetime image are seen. It is noted that there is an optical aberration that is occurring in these images that seems to show a three-dimensional flow effect. This is most likely due to a shadow caused by the window frames. This is not present in the lifetime images because the data for each ratio is collected at the same conditions, thus it cancels out. However, in this method, the conditions are slightly changed (model is not in the exact same position and the oxygen levels are not identical), therefore, this begins to manifest.

Single-Shot Lifetime Technique

For the tunnel entry at 0.3-m TCT, the more standard frame accumulation mode was employed to acquire lifetime images. As can be seen, the smaller form factor cameras (which are required for NTF) are simply too noisy to be used in this mode. Much better images can be acquired using a thermoelectrically cooled CCD camera. However, these cameras are much larger and not as robust as the smaller cameras and incorporation into NTF may not be possible.

An alternative lifetime method has been recently used for specific applications. This is the “single-shot lifetime” technique, in which both Gate 1 and Gate 2 images are acquired from a single high powered laser pulse. This technique was developed and used successfully for capturing PSP images on rotor blades [22-24]. The more traditional frame accumulation mode of lifetime imaging would require hundreds or thousands of LED flashes to acquire a single gate image, with a single flash per rotation. This was shown to suffer from excessive blurring due to flapping and lead-lag of the blade (i.e., the blade motion and timing are subtly changing with every rotation). However, replacing the LEDs with a high-powered pulse laser and operating the cameras in a “dual exposure” mode allows the accumulation of two

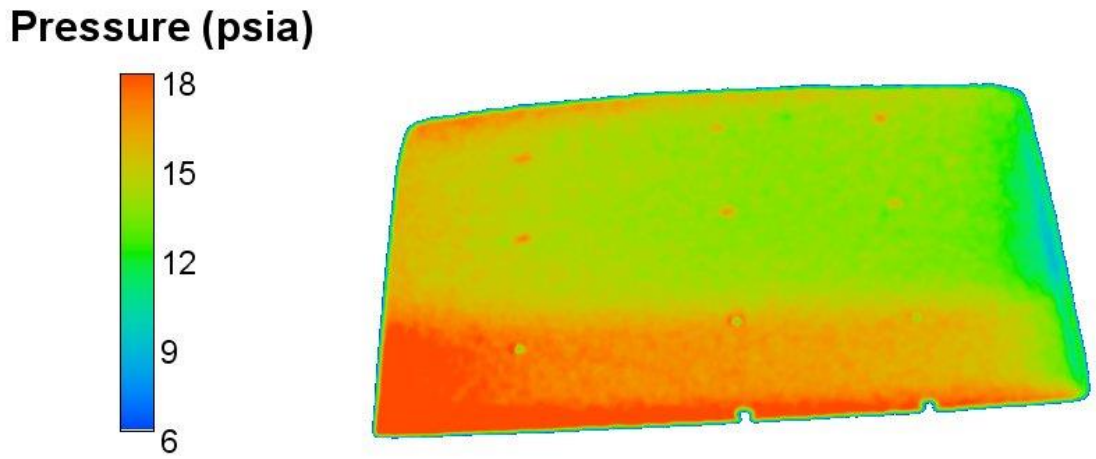

Fig. 13 Recovered pressure from CoolSNAP camera in intensity mode. Test conditions are T = 150 K, M = 0.7, AOA = 3.2 deg. Tunnel flow is from right to left in the image.

gate images from one laser pulse. Dual exposure mode is generally available in interline CCD cameras and is often used for particle imaging velocimetry experiments. In single-shot lifetime PSP, the first image is a short exposure that occurs during the less pressure sensitive initial portion of the excited-state decay, while the second image is a longer exposure capturing the remainder of the excited-state decay (which has larger pressure sensitivity). The general process of the technique is shown in Fig. 14, where Gate 1 is analogous to the "wind-off" image (and used as a reference image), and Gate 2 is analogous to the "wind-on" image. The single-shot lifetime approach has been more fully described by Gregory et al. [25] and Juliano et al. [22]

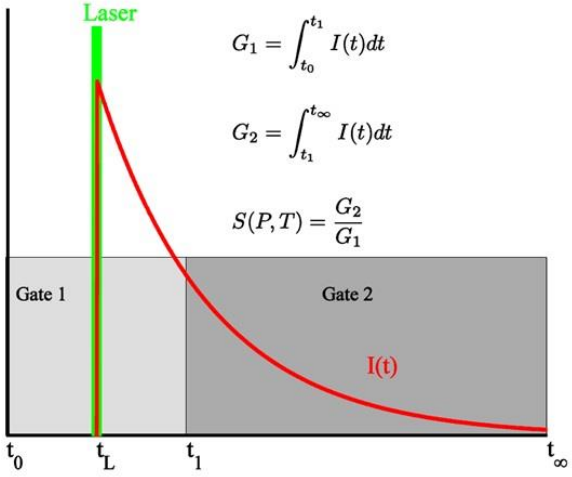

Fig. 14 Single-shot lifetime technique. Please note that the width of the gate images is not drawn to scale.

This technique was not tested in the 0.3-m TCT entry. This will require some design and development of the laser installation system as well as the beam alignment and spreading optics for the facility. However, calibrations were done using the cryogenic PSP formulation. This calibration was done using 5000 ppm O_2 in N_2 (to simulate NTF

atmospheres at higher pressures) but at ambient temperatures. This is just to show the efficacy of this technique. A typical Gate 1 and Gate 2 image are shown in Fig. 15. These are from a single laser pulse, and as can be seen, the images are quite clear and free of the shot noise that permeated the images collected with this camera in frame accumulation mode. While faint, the vertical "stripes" are still present (from the masking for the interline transfer process), but only in the Gate 2 image. The Gate 1 image is acquired without the interline transfer, so these are not present. In contrast, both gate images acquired using the frame accumulation mode employ the interline transfer of the camera, so it is present in both gate images in this mode. In addition, the stripes are quite faint in Gate 2. This is most likely because there is only one interline transfer process involved using single-shot lifetime mode, so the effect is much less.

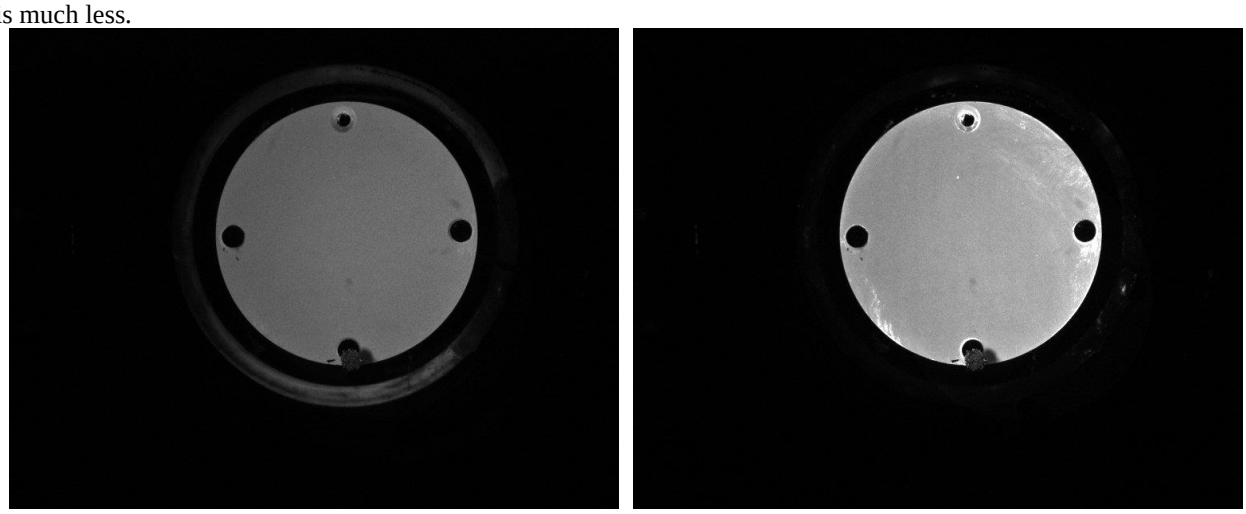

Gate 1 **Gate 2**

Fig. 15 Single-shot PSP lifetime images collected in 5000 ppm O_2 in N_2.

A comparison of the pressure sensitivity of each image as well as the sensitivity of the ratio (Gate 1/Gate 2) is shown in Fig. 16. As noted above, the pressure sensitivity of the first image (Gate 1) is significantly less than that of the second image (Gate 2). Like other lifetime techniques, this does not alleviate the need for a wind-off image (the same lifetime inhomogeneity effects are still present), but it does have some potential significant advantages over the standard frame accumulation technique. First, the same smaller cameras are employed, so no specialized image acquisition equipment is needed. Second, the shot noise is significantly reduced in this mode, as well as the vertical stripping. Finally, image pairs can be acquired at rates up to 3-4 fps. While this may not seem much, it does provide the opportunity for image averaging to further increase signal-to-noise.

More testing in the laboratory and potentially 0.3-m TCT will need to be performed using this technique. While 0.3-m TCT can provide a good small facility to test this in a similar atmosphere, the optical space is very limited. For the NTF, however, efforts have already been researched and instrumentation designed and installed for bringing in high-power laser beams for techniques such as FLEET [26, 27] For the laser-based PSP technique, these designs could be leveraged to build light paths for the high-powered pulse beams that are needed. Funding and time to build and install these are still needed, but much of the initial groundwork has already been completed.

Qualitative Skin Friction

Recent work (references from T. Liu) has shown that qualitative skin friction lines can be obtained from pressure gradients obtained using PSP. This is possible because even though skin friction and surface pressure are conventionally treated as two independent quantities, there is still an explicit coupling relationship between skin friction and surface pressures in viscous flows. This intrinsic relationship is derived from the Navier-Stokes equations and requires an approximation of the boundary enstrophy flux (BEF). A full treatment of this principle and calculations is provided by Liu *et al.* [28], Liu [29], and Liu *et al.* [30]

For cryogenic testing, this type of breakthrough could provide significant value to researchers as it provides a quantity (skin friction) that is difficult to measure in cryogenic wind tunnels. One of the more traditional approaches

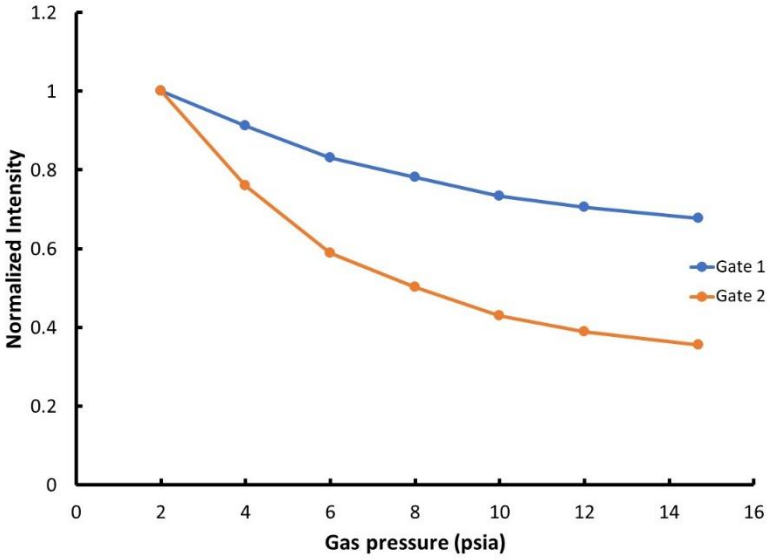

a)

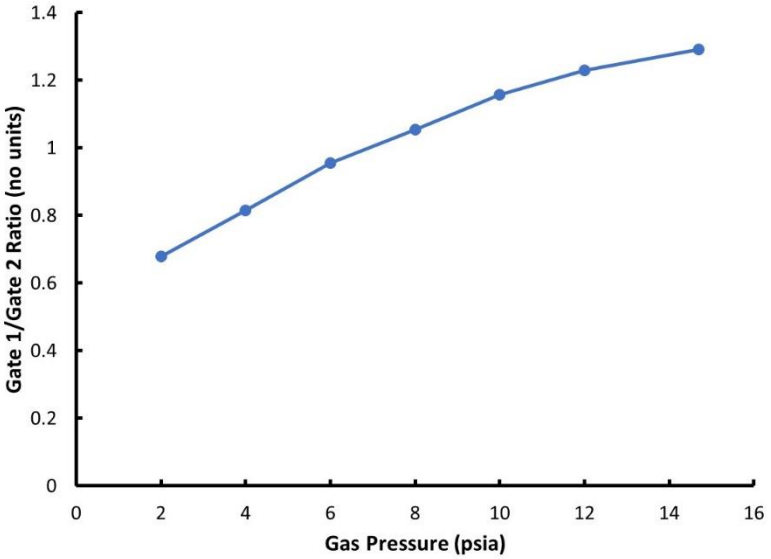

b)

Fig. 16 Calibration results from single-shot lifetime data acquisition using 5000 ppm O2 in N2. a) Normalized intensity from each image; b) Gate 1/Gate 2 ratio.

to measure global skin friction is oil film interferometry (OIF), but application of this in a facility such as the NTF has major challenges, including but not limited to the need for multiple access to the model to continually reapply the oil, identification of a suitable oil that has the desired characteristics at cryogenic conditions, and the potential for oil contamination in the facility itself. Being able to acquire this type of data using a complimentary technique (such as PSP) brings a new measurement capability that adds little to no cost in facility operations, as this data is acquired along with the PSP data. Skin friction can be calculated from temperature gradients as well, such as those collected using TSP or IR thermography [31]. Finally, these types of calculations can also be performed on legacy data that provide either surface pressure or temperature gradients.

A demonstration of this type of calculation was completed using the data presented in Fig. 13. All processing was performed by David Salazar and Professor Tianshu Liu at Western Michigan University. Currently, these types of calculations are best performed on a "flat" image, so the data in Fig. 13 was warped to be flat. This flattened image is shown in Fig. 17 with the white region of interest (ROI) box detailing the analyzed region (the portion of the region that is affected by the window frame is removed from consideration). Since this model is a simple airfoil, the spanwise-

averaged surface pressure was used to simplify the calculations and provide enhanced signal-to-noise. The normalized surface pressure is shown in Fig. 18(a). This data was then used to calculate a normalized skin friction, whose profile is shown in Fig. 18(b) and shows a thin separation region near the leading edge. A zoom-in of this region (depicted by the green box in Fig. 18(b)) is shown in Fig. 19, with the separation and attachment lines identified (SL and AL).

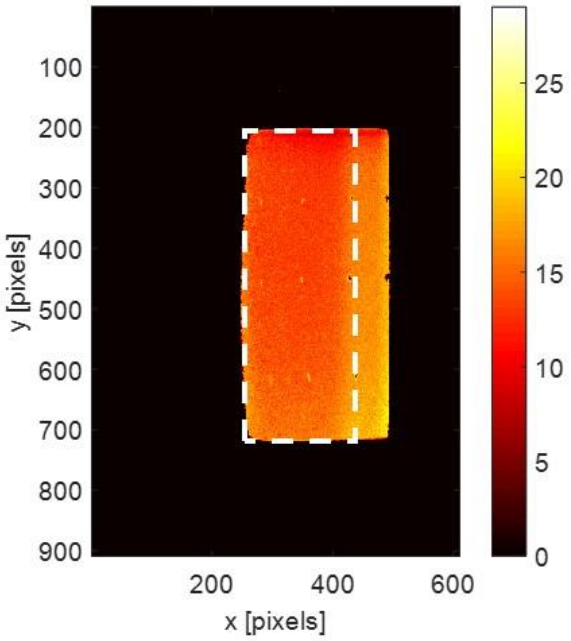

Fig. 17 Warped PSP image (Fig. 11). The white ROI box indicates the analyzed region.

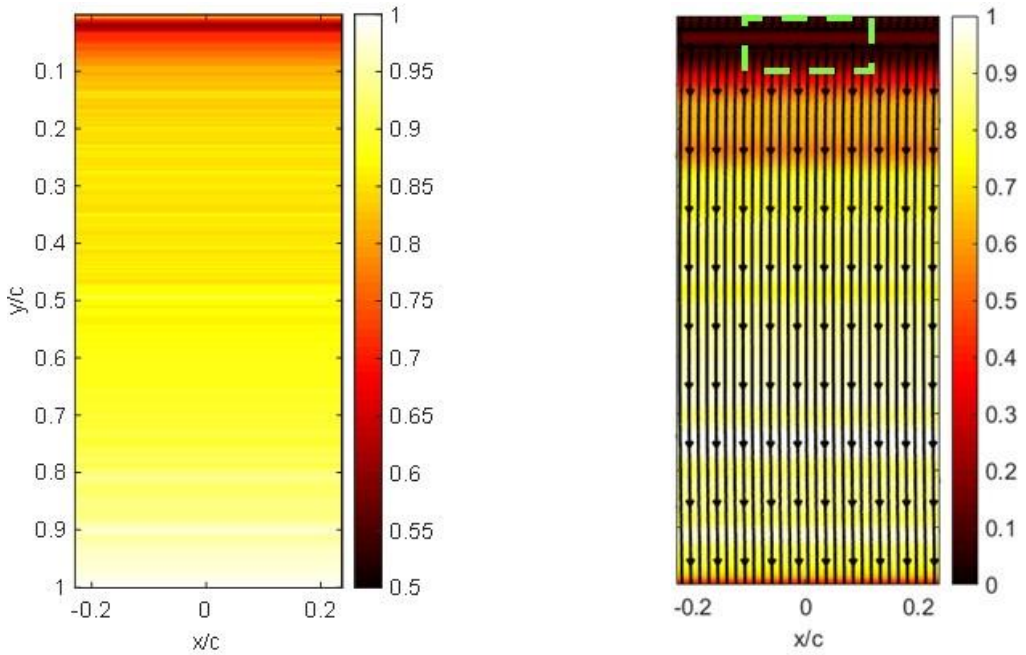

a) **b)**

Fig. 18 (a) spanwise-averaged normalized surface pressure; (b) spanwise-averaged normalized skin friction magnitude and lines.

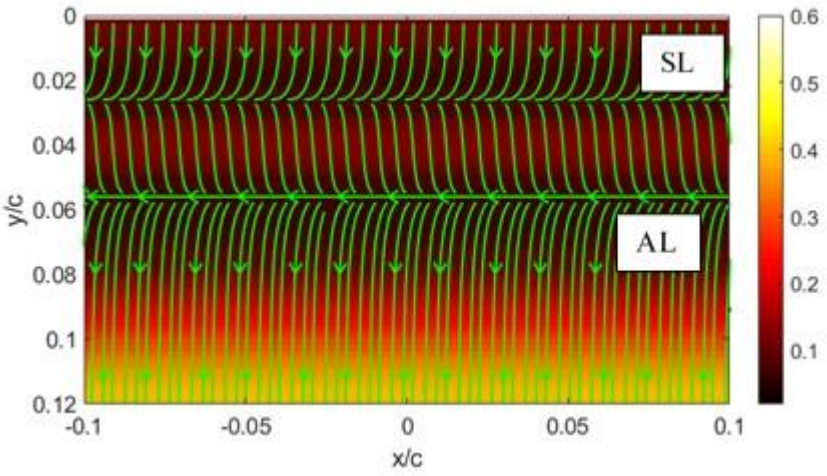

Fig. 19 Zoom-in (green box in Fig. 18(b)) of the normalized skin friction magnitude and lines with the separation line (SL) and attachment line (AL) indicated.

The calculation of skin friction based on surface pressure and temperature gradients at cryogenic conditions is currently being developed under a Small Business innovation Research (SBIR) contract (80NSSC20C0449) by Innovative Scientific Solutions, Inc. (ISSI) in partnership with Professor Tianshu Liu at Western Michigan University.

Other NTF PSP System Upgrades

A. Lighting Upgrade

Optical access for the NTF is limited to certain "ports" which can be used for things like illumination and camera placement. A figure depicting these access ports is shown in Fig. 20. In general, the ports have optical windows that are approximately 15.24 cm (6 in) in diameter. The ports themselves are cylindrical with widths ranging from 33 cm (13 in) to 53.3 cm (21 in) and the depth of 68 cm (26.75 in).

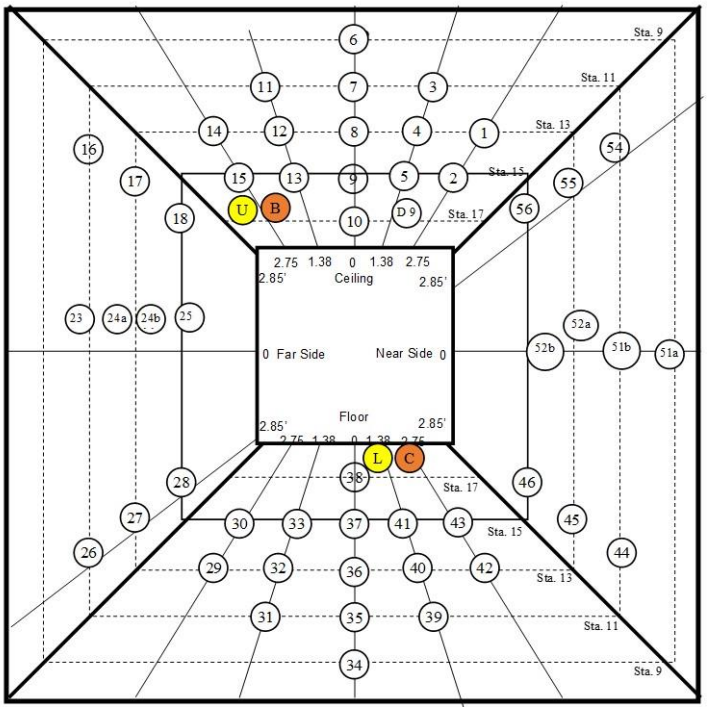

Fig. 20 Layout of the optical ports in the NTF. ports U and L are halogen lights for surveillance cameras in B and C.

For the lighting of the PSP system, the window size and port size (listed above) have been the main driver for their design. The earliest system in NTF was designed for TSP experiments to visualize flow transition on a model. This employed high powered strobe lights. For these types of experiments, these lights worked well as they could produce high powered light flashes at several Hz, and the relative instability of these lights was not a detriment for this type of testing. However, for PSP experiments, the stability of the lighting is critical, especially in low oxygen environments, where the measured change in intensity is relatively small. The ideal solution for this is to use solid-state lighting (LEDs) as they are very stable (typical drifts are ~1% per hour if the environment is constant), are relatively bright for their size and power requirements, and can be constructed to provide light at a specific wavelength with a narrow bandwidth. In the late 1990s, the invention of the blue LED made their use in PSP feasible. This was further cemented with the development of near UV LEDs, and these are currently employed by most users of PSP. Furthermore, the improvement of the technology has resulted in the ability to generate more light with fewer diodes. An example of the evolution of the LED lighting in NTF is shown in Fig. 21, with one of the original configurations on the left, and the latest configuration on the right. Each of these designs employs 400 nm LEDs that have a bandwidth of 20 nm (full width, half maximum). However, the lighting from the design on the left was able to produce about 80 W, while the newer design can produce 27 W from each die, for a total of 216 W.

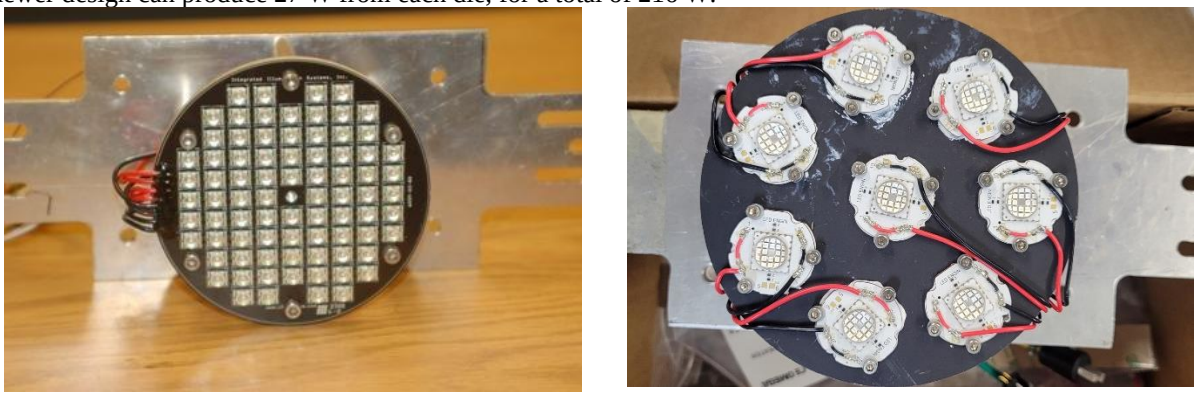

Fig. 21 (left) older version of LED lighting for NTF from Ref. 14 employing 80 LED dyes; (right) newest version of LED lighting employing 8 LED dies.

The one disadvantage of employing these solid-state lights at cryogenic conditions is that the LEDs will stop operating if the temperature is too low (the electrons cannot jump the band gap, thus no light can be produced). This was solved by adding heating to the lights. In addition, the newest generation of lights produces significantly more heat than the previous generations, thus a heat sink was added to allow them to operate effectively at warm run conditions. The initial design of the lighting with the newer LEDs was to include the heat sink and then add a heater to the cooling fins for use at cryogenic conditions. The power for the heating system was such that all of the LEDs were heated using the same source which imposed a minimum temperature limit of 172 K (-150 °F). This was deemed sufficient as it was used in the previous design (Fig. 21 (left)). Several TSP tests were performed using this design at a variety of conditions, and in general, the lighting system performed adequately.

However, a PSP test was conducted in 2021 (Test 231 – 1.75%-Scale NESC SLS Block 1 Cargo Model) and showed some significant issues with the lighting system. This was initially noticed during the tunnel cooldown as the exposure time required for PSP image continued to increase. At warmer temperatures, the exposure time was approximately 50 ms. However, at the cryogenic condition desired, the exposure time had climbed to 2 s, an increase of a factor of 40. The added increase in the exposure time also rendered several conditions unusable due to the model dynamics. At certain conditions, the model would vibrate (“buzz”), and the longer exposure times resulted in significant blur of the image. Even when these dynamics did not occur, the overall PSP results were unsatisfactory due to significant differences between the reference images and the wind-on images. A representative ratio image (slow-roll/wind-on) is shown in Fig. 22. As can be seen, there is no evidence of pressure, there is a huge background from reflections off the floor (due to the increased exposure time), and there is a gradient across the model approaching 20%.

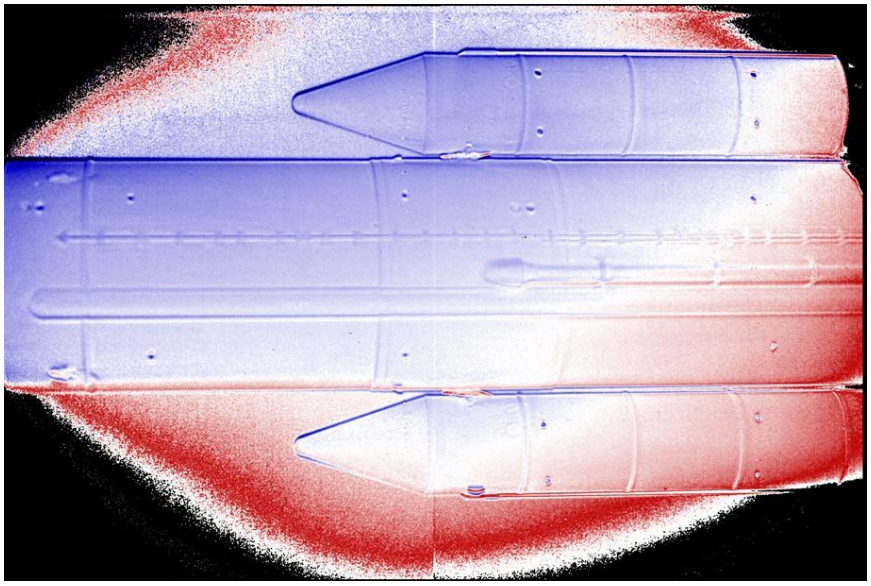

Fig. 22 Cryogenic PSP results showing significant lamp instability. Model conditions are M = 0.8, T = 116 K (-250 °F). Tunnel flow is left to right.

To explore the origin of the gradient across the model, a comparison of slow-roll images acquired both before and after a Mach 0.8 polar is shown in Fig. 23. In this case, the ratio of the images should be approximately 1. However, the maximum of the scale is 2.5 (scale bar not shown). Furthermore, the general shape of the gradient across the ratio is similar to that seen in Fig. 22. This implies that not only are the lights unstable (one reference image is larger than the other), but some lights are more unstable than others.

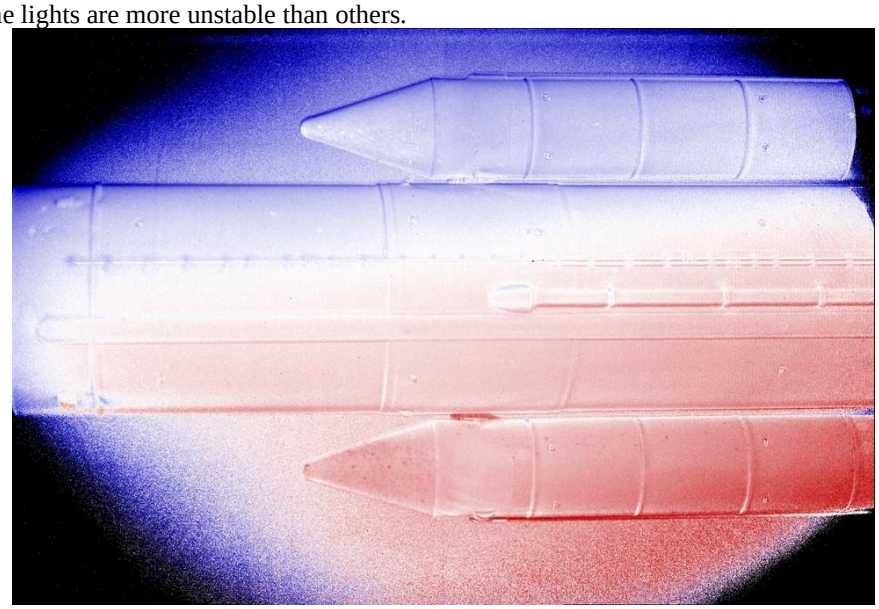

Fig. 23 Ratio of slow-roll images collected before and after a polar.

After further investigation, it was determined that over the years some of the LED lights had essentially lost all heating capability. A study of the lights was conducted after the tunnel entry. For this, a surveillance camera that was already in place and could observe two LED pods was employed. The LED lights were chosen so that one LED was heated using a modified heating method (described below) and one was heated using the traditional setup. A representative image with labelled LED pods is shown in Fig. 24(a) and the light output as a function of the NTF structure temperature and the temperature measured with a resistance temperature detector (RTD) on the back of the LED pod is shown in Fig. 24(b) and Fig. 24(c), respectively. The results of this test showed that when the temperature

of the traditionally heated light was decreased below ambient, the intensity began to decrease and eventually was nearly indistinguishable from the background.

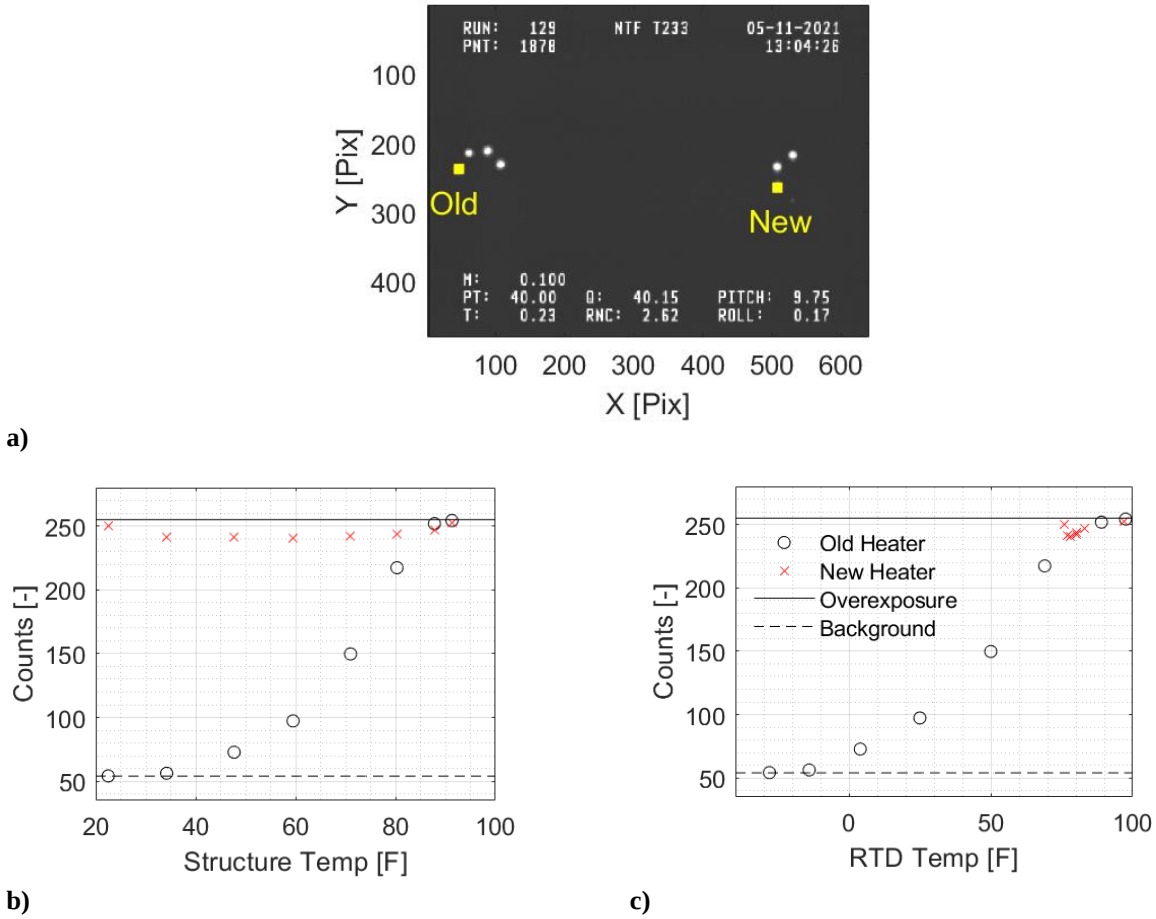

Fig. 24 a) Surveillance camera image showing the LED pods that were investigated. The pods are labelled "New" for the newer heating method and "Old" for the traditional heating method; b) the light output from the traditional heating method (Old Heater) and improved method (New Heater) as a function of NTF structure temperature; c) the same output as a function of the temperature as measured by RTDs on the back of the LED pods.

Due to the nature of the camera, the decrease is most likely more than a factor of 5 as the camera was mostly saturated until the decrease. Similarly, for the LED with the newer heating method, only a small drop in the output was observed, though again, the camera that was available was mostly saturated at higher LED temperatures. Regardless, this test did show that there were significant issues with the way the LEDs have been heated. It was noted that the lights themselves are not placed in an environmental chamber of any sort (due to the space limitations of the NTF ports), thus they are directly experiencing the flow around it. Not only is this accounting for the intensity loss, but it could also be driving the instability, as the higher flow conditions should be cooling the lights more effectively than the slower conditions that are used for reference images. For the TSP testing that was done previously, this issue was very minor for a few reasons. The TSP is generally brighter (several factors) than the PSP, and all of the TSP data was taken over a short period of time (*e.g.*, during a short temperature step lasting about 30 s). Thus, the instability and loss of intensity of the lamps was not a big factor.

To address these lighting issues, the current design is being modified in two ways. First, the heat sink was removed from the back of the LEDs. While this will require some adjustment for warm runs, it should greatly increase the heating efficiency since the LEDs will be heated directly. Second, each heater is now controlled independently (initially it was one heater circuit for all LED lights) and the setpoint has been increased to 300 K (80 °F). Currently, all of the LED lights are being modified for this type of operation and a full test of the system is scheduled for Spring 2023.

Paint Application

The traditional application of PSP for cryogenic conditions was investigated in the laboratory. Many of the models that are cryogenically tested are designed to have mirror finishes to reduce the effects of surface roughness. At cryogenic conditions, however, it can be very difficult to apply coatings that will stick to the surface. With this in mind, it was determined that specific underlayers and basecoats were needed to promote adhesion of the PSP to the model. These paint applications take about 24 hours if heating is employed to facilitate faster curing, and 2-3 days if the undercoat and base coat are allowed to cure without heat. The steps for applying the traditional cryogenic PSP are shown in Fig. 25.

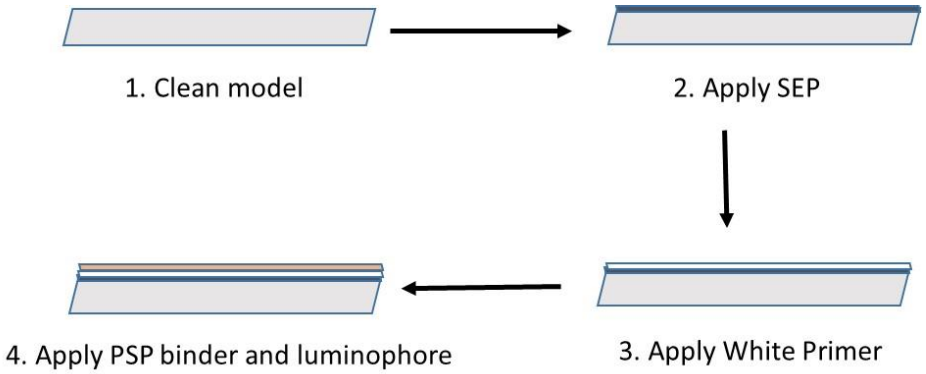

Fig. 25 Steps for applying traditional cryogenic PSP. SEP is the self-etching primer undercoat to promote adhesion of the basecoat and PSP binder.

In initial tests, it was shown that the application of the undercoat and basecoat could be done outside of the tunnel or done in place (to allow purging the pressure ports) before the tunnel cooldown occurs. However, in a later test, following this procedure showed deleterious effects (as shown in Fig. 26). In this test, the cryogenic PSP was applied in place but before tunnel cool down. After purging the tunnel (which requires several runs at high speed and pressure), the tunnel was then cooled to the operating temperature. During this process, something happened to cause what looked like permanent turbulent wedges to appear. This was done several times and showed a similar effect. The only solution that was shown to be viable was to either apply all coatings in place after the tunnel cooled down (resulting in at least 2 shifts of the tunnel being at cryogenic condition with the access housing in place) or painting the basecoat before operation, purge and cool down the tunnel, then apply the PSP coating in the access housing. If this method is chosen, cleaning of the basecoat is essential to remove any contaminants that may be present from the purge and cool down process.

Fig. 26 Slow-roll cryogenic PSP image showing permanent turbulent wedges

One of the other drawbacks to this type of PSP application is that the test matrix must be determined with care. If any information from a “clean” model (i.e., no paint applied) is desired, then this must be taken into account. In this case, if PSP is run first, several days must be allowed to remove the paint, with possible damage done to other instrumentation in the model (even with purging pressure taps). If this is done at cryogenic conditions, then a decision to either remove the model or do this in the access housing must be made. If it is desired to run the clean model first,

then sufficient time must be allotted to paint the model, as well as either removing the model or painting in the access housing. Recently, experiments at DLR [15, 32] have shown that the cryogenic PSP can be directly applied to a model surface. This was also tested at the NTF by applying the cryogenic PSP directly to the sting (Fig. 27 (left)) and directly to a metal model (Fig. 27 (right)) and neither showed significant degradation. From laboratory testing, it was determined that the cryogenic PSP can be applied either with or without the TiO_2, which is used as a white pigment. Having the white pigment can help to significantly hide any defects or other features on the model that can interfere with PSP imaging, as well as provides much greater return of the luminescent signal. However, adding the TiO_2 does require the pressure taps to be purged. If the TiO_2 is omitted, there is a decrease in signal, but the taps do not need to be purged and the resulting layer is usually thinner. Additional laboratory tests need to be completed to more fully characterize the best way to apply the cryogenic PSP.

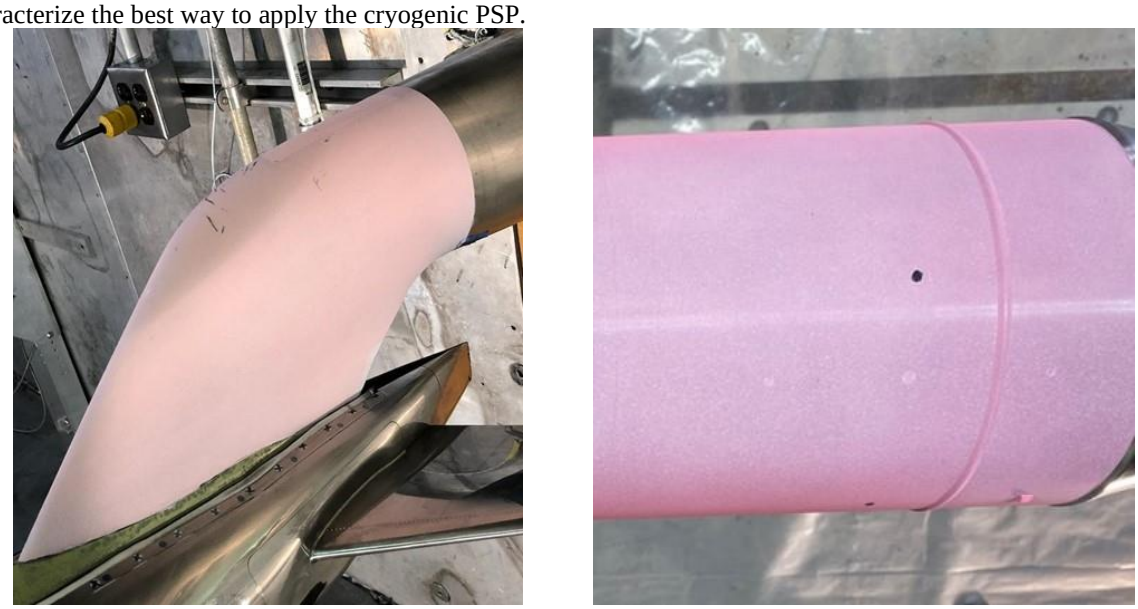

Fig. 27 (left) Application of cryogenic PSP directly to the sting in NTF; (right) application directly to a metal model.

Conclusions, Recommendations, and Future Efforts

A. Lifetime Acquisition

The results from the 0.3-m TCT entry can lead to several conclusions about the use of lifetime data acquisition in the NTF. First, the PSP-CCD-M cameras are too noisy in the frame accumulation mode to provide adequate images for PSP analysis. The main limitation in these cameras is the lack of thermoelectric cooling. Even taking care to subtract background images does not completely minimize the noise. The capability of the camera to thermoelectrically cool the chip reduces the shot noise significantly, as demonstrated with the CoolSNAP HQ camera. Regardless, even images collected with CoolSNAP HQ camera displayed more noise that the more traditional wind-on/slow-roll acquisition method currently in use. This is due to non-heterogeneity of the lifetime in the paint due to uneven application and other factors that are difficult if not impossible to control, especially if complex models (other than simple airfoils) are to be tested. While these types of effects are usually present in all lifetime testing, this is exacerbated when low signal changes are present, such as in oxygen poor and cryogenic environments. To account for this requires a pair of images at a wind-off or slow-roll condition. Thus, the lifetime data acquisition method at NTF will not alleviate the need for wind-off reference images to be collected.

If the traditional lifetime data acquisition is to be pursued, then there will be a need to be a complete redesign of the LED lighting system that is currently in place. This system is designed to provide stable high intensity light in a constant illumination mode. However, the frame accumulation mode requires the LEDs to be able to pulse at relatively high repetition rates (on the order of up to several kHz) with narrow pulse widths (usually 30 μs or less). In addition, the LED pulse must have a very short rise and fall time (typically < 1 μs). There are commercially available units for doing more traditional tests (e.g., Innovative Scientific Solutions, Inc. sells a variety of LED-based power supplies for lifetime applications). Unfortunately, these components are made to be used in conditions closer to ambient pressure

and temperature. The electronic components that are employed will not handle the cryogenic temperature or high pressures experienced in the NTF. There are potentially three solutions available:

1) Completely redesign the lighting to handle the temperature and pressures in the plenum, or
2) Build suitable environmental chambers for the commercially available units to maintain ambient pressure and temperature, or
3) Have a company design and build the units, possibly using the SBIR mechanism.

Regardless of the choice, significant time and expense may be required to accomplish this.

Implementing the single-shot lifetime approach may be a better option if a lifetime technique is desired. Currently existing cameras will operate in this mode and provide the ability for image averaging that the frame accumulation method does not. Overall, it does provide better signal-to-noise, though more laboratory testing at cryogenic conditions still needs to be done. If implemented into the NTF, then existing designs for the high-powered laser entry ways used for FLEET can be leveraged as well.

Camera Selection

While the results from the 0.3-m TCT entry provide significant insight into the performance of the types of cameras chosen, selection of which camera to use in the NTF has to be based on other criteria as well. While it has been shown that the scientific-grade CCD camera (the CoolSNAP HQ) performs better overall than the smaller camera, the size difference alone will preclude its use in the NTF. This is shown in more detail in Fig. 28, which is a photograph of the respective camera systems with requisite power supply. It does not include additional equipment, such as fiber optic converters. As can be seen, the size requirements of the CoolSNAP are much higher than the requirements for the PSP-CCD-M camera. To put this in perspective, photographs for the current camera housing (which only provides heating for the camera) are shown in Fig. 29.

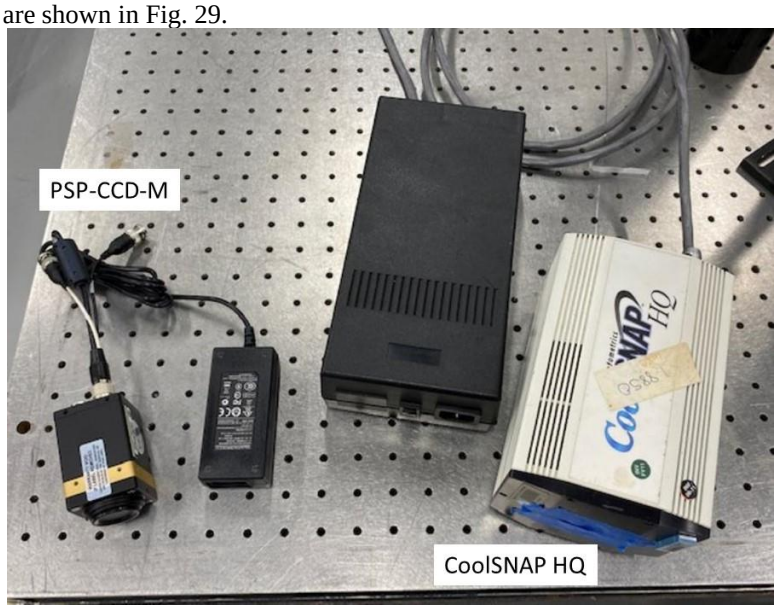

Fig. 28 Photograph of the PSP-CCD-M camera and associated power supply compared with the CoolSNAP HQ camera and its power supply.

Fig. 29 Photographs of the current camera housing.

There is one final point to consider. Most companies that have produced much of the scientific-grade cameras as well as higher end machine vision cameras have stopped manufacturing CCD cameras and changed to CMOS cameras. While there are several advantages to using CMOS cameras, there are currently no CMOS cameras that have the frame accumulation mode. This is a looming problem for many of the current PSP users who have been using frame accumulation cameras, with users having to purchase cameras from used scientific vendors and have them refurbished for use. For the single-shot lifetime technique, the prospects are a bit better, with some CMOS cameras capable of operating in interline transfer mode with interline transfer times on the order of 100-200 ns (e.g., the Imager sCMOS CLHS camera from LaVision (https://www.lavision.de/en/products/cameras/cameras-for-piv/index.php)), however, these cameras have not been evaluated for the single-shot lifetime PSP method.

Regardless of the availability of the frame accumulation mode CCD cameras, if this type of camera is chosen, it is highly recommended that a suitable environmental chamber be developed for use in the ports of the NTF. The initial cameras employed in the NTF system were scientific grade CCDs. Most of these CCDs have a thin coverslip over the CCD chip. This allows the CCD chip to be housed in a small vacuum to help decrease the noise. In addition, if the chip is thermoelectrically cooled (as is the case of the CoolSNAP camera, which is cooled to 243 K), then this cover slip is vital to keep condensation from forming on the CCD chip, possibly resulting in damage or chip failure. With the cameras in the early version of the system, the pressure environment in the NTF could cause these coverslips to crack. Having the cameras in an environmental chamber that can provide both heat (for the camera to function properly) as well as keep the pressure near ambient (by using dry air), would protect these units from damage.

Future Efforts

While this report was focused mainly on the possibility of using lifetime data acquisition in NTF as well as current efforts to improve the existing system, several efforts are planned or already underway to improve PSP for oxygen poor environments, with an emphasis on cryogenic applications. Several of these areas have been briefly mentioned above, and some are still being developed. Below is a brief description of some of these activities:

1) Fully evaluating the application of the cryogenic PSP directly to the model surface. This has been done a few times at NTF, but still needs to be fully evaluated in the laboratory. This includes evaluating the addition of TiO_2 to the binder (which will vastly enhance signal return but is there a detriment to the performance of the PSP), evaluating the capability to smooth the paint, and the general longevity of the PSP (in terms of how long it can be used).
2) Improvements to the cryogenic PSP formulation. While there is generally only one binder that has the oxygen diffusion to show appreciable sensitivity at cryogenic conditions, other improvements are being investigated. These include evaluating different types of TiO_2 to determine if factors such as degradation of the paint aging of the PSP can be curtailed by using a different type of TiO_2 (there are many different types of TiO_2 that have different coatings for different applications), the addition of a second dye to help correct errors that arise with using a reference image, etc.
3) Evaluating the ability of using the cryogenic PSP as a time-resolved PSP. Time-resolved PSP (or unsteady PSP, uPSP) is a technique that has been seeing an increased amount of use due to the technology advances in both the lighting as well as the CMOS high speed cameras. Cryogenic PSP has been demonstrated by researchers at DLR [32] in the Cryogenic Ludweig-Tube Göttingen (KRG). However, implementation in the NTF will introduce significant challenges, including identifying a suitable camera and developing suitable data acquisition procedures to name a few.

4) Full implementation of the skin surface friction calculation from surface pressure and/or temperature distributions. This will come through a current SBIR contract (ISSI, 80NSSC21C0547), and further evaluation will be performed on upcoming tests scheduled for 2023.

Some of these pathways will also benefit the standard uPSP in the Transonic Dynamics Tunnel (TDT). This facility operates in an atmosphere of R-134A (a refrigerant) so has some of the same challenges as far as oxygen poor environments. A separate report detailing the ongoing testing of uPSP in the TDT will be forthcoming in 2023.

Acknowledgments

This report is the culmination of several years of research and testing with the assistance of many people. Kyle Goodman (Analytical Mechanics Associates) and Sarah Peak (National Institute of Aerospace) are an integral part of the PSP team and have conducted or assisted in all of the research and testing presented here. Cliff Obara, Mike Chambers, Tami Price, Karl Maddux, and Reginald Brown are the test engineers and technicians who assisted with the 0.3-m TCT tunnel entry. Finally, the authors wish to acknowledge the entire staff of the NTF, especially the instrumentation technicians James "Monty" Montgomery and William "Bill" Dressler. Funding for this work has been provided by the Innovative Measurements subproject of the Transformational Tools and Technologies program of NASA.

References

[1] Kilgore, R.A. and Dress, D.A., "The Application of Cryogenics to High Reynolds Number Testing in Wind Tunnels. Part 1: Evolution, Theory, and Advantages," *Cryogenics*, Vol. 24, No. 8, 1984, pp. 395-402. doi: 10.1016/0011-2275(84)90011-0

[2] Kavandi, J., Callis, J., Gouterman, M., Khalil, G., Wright, D., Green, E., Burns, D., and McLachlan, B., "Luminescent Barometry in Wind Tunnels," *Review of Scientific Instrumentation*, Vol. 61, No. 11, 1990, pp. 3340-3347. doi: 10.1063/1.1141632

[3] Morris, M.J., Benne, M.E., Crites, R.C., and Donovan, J.F., "Aerodynamic Measurements Based on Photoluminescence," AIAA Paper 93-0175, 1993. doi: 10.2514/6.1993-175

[4] McLachlan, B., and Bell, J., "Pressure-Sensitive Paint in Aerodynamic Testing," *Experimental Thermal and Fluid Science*, Vol. 10, No. 4, 1995, pp. 470-485. doi: 10.1016/0894-1777(94)00123-P

[5] Liu. T., Campbell, B., Burns, S., and Sullivan, J., "Temperature- and Pressure-Sensitive Luminescent Paints in Aerodynamics," *Applied Mechanics Reviews*, Vol. 50, No. 4, 1997, pp. 227-246. doi: 10.1115/1.3101703

[6] Liu, T., and Sullivan, J., *Pressure and Temperature Sensitive Paints (Experimental Fluid Dynamics)*, Springer-Verlag, Berlin, 2005, pp. 1-36.

[7] Lakowicz, J., *Principles of Fluorescence Spectroscopy, 2nd ed.*, Kluwer Academic/Plenum Publishers, New York, 1999, pp. 239-242.

[8] Upchurch, B.T. and Oglesby, D.M., "New PSP Developments at NASA Langley Research Center – Low Temperature PSP," *Proceedings of the 6th Annual Pressure Sensitive Paint Workshop*, Seattle, Washington, 1998, pp. 10-1 – 10-24.

[9] Asai, K., Amao, Y., Iijima, Y., Okura, I., and Nishide, H., "Novel Pressure-Sensitive Paint for Cryogenic and Unsteady Wind Tunnel Testing," AIAA Paper 2000-2527, 2000. doi: 10.2514/6.2000-2527

[10] Asai, K., Amao, Y., Iijima, Y., Okura, I., and Nishide, H., "Novel Pressure-Sensitive Paint for Cryogenic and Unsteady Wind-Tunnel Testing," *Journal of Thermophysics and Heat Transfer*, Vol. 16, No. 1, 2002, pp. 109-115. doi: 10.2514/2.6658

[11] Masuda, T., Isobe, E., and Higashimura, T., "Poly[1-(trimethylsilyl)-1-propyne]: A New Polymer Synthesized with Transition-Metal Catalysts and Characterized by Extremely High Gas Permeability," *Journal of the American Chemical Society*, Vol. 105, No. 25, 1983, pp. 7473-7474. doi: 10.1021/ja00363a061

[12] Watkins, A.N., Leighty, B.D., Lipford, W.E., and Goodman, K.Z., "Pressure- and Temperature-Sensitive Paint at 0.3-m Transonic Cryogenic Tunnel," NASA TM NASA-2015-218801, 2015.

[13] Watkins, A.N., Goad, W.K., Obara, C.J., Sprinkle, D.R., Campbell, R.L., Carter, M.B., Pendergraft, O.C., Bell, J.H., Ingram, J.L., Oglesby, D.M., Underwood, P.J., and Humber, L.R., "Flow Visualization at Cryogenic Conditions Using a Modified Pressure Sensitive Paint Approach," AIAA Paper 2005-456, 2005. doi: 10.2514/6.2005-456

[14] Watkins, A. N., Leighty, B.D., Lipford, W.E., Oglesby, D.M., Goodman, K.Z., Goad, W.K., Goad, L.R., and Massey, E.A., "The Development and Implementation of a Cryogenic Pressure Sensitive Paint System in the National Transonic Facility," AIAA Paper 2009-421, 2009. doi: 10.2514/6.2009-421

[15] Yorita, D., Klein, C., Henne, U., Ondrus, V., BEifuss, U., Hensch, A-K., Longo, R., Guntermann, P, and Quest, J., "Successful Application of Cryogenic Pressure Sensitive Paint Technique at ETW," AIAA Paper 2018-1136, 2018.
doi: 10.2514,6.2018-1136
[16] Kilgore, R.A., Goodyear, M.J., Adcock, J.B., and Davenport, E.E., "The Cryogenic Wind Tunnel Concept for High Reynolds Number Testing," NASA TN NASA-TN-D-7762, 1976.
[17] Kilgore, R.A., "Design Features and Operational Characteristics of the Langley 0.3-Meter Transonic Cryogenic Tunnel," National Technical Information Service, Alexandria, VA, USA, 1976.
[18] Burner, A.W. and Goad, W.K., "Flow Visualization in a Cryogenic Wind Tunnel Using Holography," NASA TM NASA-TM-84556, 1982.
[19] Johnson, W.G., Hill, A.S., and Eichman, O., "High Reynolds Number Tests of a NASA SC(3)-0712(B) Airfoil in the Langley 0.3-Meter Transonic Cryogenic Tunnel," NASA TM NASA-TM-86371, 1985.
[20] Sellers, M.E., "Demonstration of a Temperature-Compensated Pressure Sensitive Paint on the Orion Launch Abort Vehicle," AIAA Paper AIAA-2011-3166, 2011.
doi: 10.2514/6.2011-3166
[21] Watkins, A.N., Jordan, J.D., Leighty, B.D., Ingram, J.L., and Oglesby, D.M., "Development of Next Generation Lifetime PSP Imaging Systems, *Proceedings of the 20th International Congress on Instrumentation in Aerospace Simulation Facilities*, IEEE, 2003, pp. 372-382.
doi: 10.1109/ICIASF.2003.1274889
[22] Juliano, T.J., Kumar, P., Ping, D., Gregory, J.W., Crafton, J., and Fonov, S., "Single-Shot, Lifetime-Based Pressure-Sensitive Paint for Rotating Blades," *Measurement Science and Technology*, Vol. 22, No. 8, 2011, 085403 (10 pp.)
doi: 10.1008/0957-0233/22/8/085403
[23] Watkins, A.N., Leighty, B.D., Lipford, W.E., Wong, O.D., Goodman, K.Z., Crafton, and Gregory, J.W., "Measuring Surface Pressures on Rotor Blades Using Pressure-Sensitive Paint," *AIAA Journal*, Vol. 54, No. 1, 2016, pp. 206-215.
doi: 10.2514/1.J054191
[24] Weiss, A., Geisler, R., Schwermer, T., Yorita, D., Henne, U., Klein, C., and Raffel, M., "Single-Shot Pressure-Sensitive Paint Lifetime Measurements on Fast Rotating Blades using an Optimized Double-Shutter Technique," *Experiments in Fluids*, Vol. 58, No. 9 (120), 2017, 20 pp.
doi: 10.1007/s00348-017-2400-4
[25] Gregory, J.W., Kumar, P., Peng, D., Fonov, S., Crafton, J., and Liu, T., "Integrated Optical Measurement Techniques for Investigations of Fluid-Structure Interactions," AIAA Paper 2009-4044, 2009.
doi: 10.2514/6.2009-4044
[26] Reese, D.T., Thompson, R.J., Burns, R.A. and Danehy, P.M., "Application of Femtosecond-Laser Tagging for Unseeded Velocimetry in a Large-Scale Transonic Cryogenic Wind Tunnel," *Experiments in Fluids*, Vol. 62, Article 99, 2021.
doi: 10.1007/s00348-021-03191-x
[27] Reese, D.T., Burns, R.A., Danehy, P.M., Walker, E.L., and Goad, W.K., "Implementation of Pulsed-Laser Measurement System in the National Transonic Facility," AIAA Paper AIAA-2019-3380, 2019.
doi: 10.2514/6.2019-3380
[28] Liu, T., Misaka, T., Asai, K., Obayashi, S., and Wu, J.Z., "Feasibility of Skin Friction Diagnostics Based on Surface Pressure Gradient Field," *Measurement Science and Technology*, Vol. 27, No. 12, 2016, 125304 (16 pp.)
doi: 10.1088/0957-0233/27/12/125304
[29] Liu, T., "Skin-Friction and Surface-Pressure Structures in Near-Wall Flows," *AIAA Journal*, Vol. 56, No. 10, 2018, pp. 3887-3896.
doi: 10.2514/1.J057216
[30] Liu, T., Salazar, D.M., Crafton, J., Rogoshchenkov, N., Ryan, C., Woike, M.R., and Davis, D.O., "Skin Friction Extracted from Surface Pressure in Incident Shock-Wave/Boundary-Layer Interaction," *AIAA Journal*, Vol. 59, No. 10, 2021, pp. 3910-3922.
doi: 10.2514/1.J060345
[31] Liu, T., "Extraction of Skin-Friction Fields from Surface Flow Visualizations as an Inverse Problem," *Measurement Science and Technology*, Vol. 24, No. 12, 2013, 124004 (18 pp.)
doi: 10.1088/0957-0233/24/12/124004
[32] Klein, C., Yorita, D., Henne, U., Kleindienst, T., Koch, S., and Ondrus, V., "Unsteady Pressure Measurements by Means of PSP in Cryogenic Conditions," AIAA Paper AIAA-2020-0122, 2020.
doi: 10.2514/6.2020-0122